



ISSN NO. 2320-5407

Journal homepage: <http://www.journalijar.com>
Journal DOI: [10.21474/IJAR01](https://doi.org/10.21474/IJAR01)

INTERNATIONAL JOURNAL
OF ADVANCED RESEARCH

RESEARCH ARTICLE

SYNTHESIS, SPECTROSCOPY, STRUCTURAL AND BIOLOGICAL STUDIES OF Hg(II), Mn(II) AND Co(II) COMPLEXES OF COUMARIN DERIVATIVES.

Rania Zaky*, Yasmineen G. Abou El-Reash, Ahmed Fekri, Hany M. Youssef, Abdulrahman S. Noori.

Department of Chemistry, Faculty of Science, Mansoura University, Mansoura, Egypt.

Manuscript Info

Manuscript History:

Received: 14 April 2016
Final Accepted: 19 May 2016
Published Online: June 2016

Key words:

Hydrazone complexes, DFT, Ion-flotation, Anti-oxidant.

Abstract

A series of Hg(II), Mn(II) and Co(II) complexes with 3-(2-(2-oxo-2H-chromene-3-carbonyl)hydrazono)-N-(pyridin-2-yl)butanamide (H₂L) were synthesised. The synthesized compounds were deduced by various spectroscopic techniques. The geometry of isolated complexes was estimated by using the DFT theory. Also, Pb(II) and Cd(II) were separated by means of flotation technique. Moreover, cytotoxic, antimicrobial and anti-oxidant activities of the synthesized compounds were examined.

*Corresponding Author

Rania Zaky.

Copy Right, IJAR, 2016,. All rights reserved.

Introduction:-

Coumarin was used in a wide-ranging in the pharmacological manufacturing as a pioneer reagent in the production of some synthetic anticoagulant drugs such as dicoumarol. Although, coumarin alone has not any anticoagulant properties it was converted into the natural anticoagulant dicoumarol via a numeral of fungi species. Dicoumarol material was accountable for sweet clover disease in the cattle eating moldy sweet clover silage [1, 2]. Also, coumarin has anti-fungal, anti-bacterial and anti-tumor activities and properties [3, 4].

Coumarin derivatives are actual good complexing agent since it has powerful binding sites for complexation with transition metal ions. This complexes were played a significant role in pharmaceuticals chemistry as well as with coordination chemistry [5]. Moreover, coumarin derivatives used in analytical chemistry as a choosy metal extracting agents. Wherever, there are several techniques such as column extraction, ion-flotation, co-precipitation, ion-selective electrode, cloud point extraction, solid phase extraction and liquid-liquid extraction were used in separation and preconcentration of some trace metal [6-10]. The ion-flotation method attracted a significant attention of researchers because of it was considered an economy, simple, efficient and speedy quantitative process [11-15].

In continuously of our work, Hg(II), Mn(II) and Co(II) complexes of 3-(2-(2-oxo-2H-chromene-3-carbonyl)hydrazono)-N-(pyridin-2-yl)butanamide were prepared and characterized [16-20]. The manner of complexation was interpreted via numerous spectroscopic and physical methods. Also, the biological activity of the isolated compounds were tested.

Experimental:-

Materials and reagents:-

All materials and reagents used are pure (Merck, Sigma or Aldrich). They included:

- Organic substance; 2-oxo-2H-chromene-3-carbohydrazide and 3-oxo-N-(pyridin-2-yl)butanamide, HOL (oleic acid).
- Metal salts; [Co(CH₃COO)₂].4H₂O, [CdCl₂].2H₂O, MnCl₂.2H₂O, HgCl₂ and Pb(NO₃)₂.
- Solvents; Absolute ethyl alcohol, dimethyl formamide and diethyl ether.

Solutions:-

A stock solution of: (a) HOL (oleic acid) ($6.36 \times 10^{-2} \text{ mol.L}^{-1}$) were prepared by dissolving 20 mL in one liter of kerosene; (b) $\text{CdCl}_2 \cdot \text{H}_2\text{O}$ and $\text{Pb}(\text{NO}_3)_2$ ($1 \times 10^{-2} \text{ mol.L}^{-1}$) were prepared in 100 ml bidistilled water; (c) $1 \times 10^{-2} \text{ mol.L}^{-1}$ of ligand was prepared in 100 ml absolute ethanol.

Instrumentation:-

Purpose	Apparatus
- Detect the infra-red spectrum	The FTIR spectrophotometer Mattson 5000, Madison, USA (range 4,000–400 cm^{-1})
- Record the ^1H NMR spectrum	The EM-390 (200 MHz) on a Varian Mercury-300 instrument (Switzerland)
- Record the MS	The Mattson 5000 FTIR spectrophotometer
- pH measurements	The pH meter "Hanna instrument 8519 digital"
- Evaluate values of magnetic moment at RT ($25 \pm 1^\circ\text{C}$)	The magnetic susceptibility balance "Johnson Matthey Wayne, Pennsylvania, USA"
- Record the UV-vis.	The spectrophotometer Shimadzu UV 240 (P/N 204-58000) (USA) in the range 200–900 nm
- Determinations the analytes concentration	GBC, Sensaa Series Atomic Absorption Spectrometry (computerized AAS) with air-acetylene flame
- Flotation and separation detection	Two types of cells which are cylindrical tube of (29, 45) cm length and (1.2, 6) cm inner diameter with a stopper at the top
- Determination the % of (C, H and N)	The "Perkin-Elmer 2400 Series II Analyzer"

Synthesis of H_2L :-

The H_2L was produced by adding of 2-oxo-2H-chromene-3-carbohydrazide (2.04gm) to 3-oxo-N-(pyridin-2-yl)butanamide (1.78 gm) in 30 ml ethanol in existence of glacial acid(1 ml). The reaction mixture were stirred for 4 h (Scheme 1). The formed precipitate were filtrated and recrystallized from absolute alcohol.

Scheme 1:- The outline of the synthesis of ligand (H_2L) and its metal complexes.
Synthesis of metal complexes:-

The isolated solid complexes were synthesized by addition equimolar amounts of ligand (H₂L) with hot ethanolic and/or aqueous solution of chloride salt of Hg(II) and Mn(II); acetate salt of Co(II). The mixture was heated on a water bath for 3 h. The formed precipitate was filtered off, washed away with hot ethanol. The physical and analytical properties were recorded in Table 1.

Table 1:- Elemental analysis and physical data of H₂L and its metal complexes.

No.	Compound	Formula	M.Wt.	Color	Yield	m.p.	Found (Calculated)				
							C	H	N	M	Cl
1	H ₂ L	C ₁₉ H ₁₆ O ₄ N ₄	364.74	Pale Yellow	80	270	62.51 (62.57)	4.39 (4.42)	15.91 (15.46)	-	-
2	[Hg(H ₂ L)(H ₂ O) ₂ Cl ₂]	HgC ₁₉ H ₂₀ N ₄ O ₆ Cl ₂	672.369	Yellowish white	75	300>	33.89 (33.94)	3.02 (2.99)	8.37 (8.33)	29.92 (29.83)	10.60 (10.56)
3	[Mn(H ₂ L)(H ₂ O)Cl ₂]	MnC ₁₉ H ₁₈ N ₄ O ₅ Cl ₂	508.694	buff	70	300>	44.81 (44.86)	3.59 (3.57)	11.02 (11.13)	10.82 (10.79)	13.93 (13.96)
4	[Co(HL)(OAc)(H ₂ O)].2H ₂ O	CoC ₂₁ H ₂₄ O ₉ N ₄	535.7523	brown	85	300>	46.89 (47.08)	4.37 (4.52)	10.49 (10.46)	11.03 (10.99)	-

Molecular modeling:-

The DFT method used to predict the geometry of the isolated complexes via the GAUSSIAN 09 program package by using DMOL3 program in Materials Studio package [21, 22]. The DNP basis sets are of analogous class to 6-31G Gaussian basis sets [23]. The DNP basis sets more accurate than Gaussian basis sets of the identical size [24]. The best brilliant exchange-correlation functional was measured based on the GGA and RPBE functional [25, 26].

Antibacterial and antifungal activities in terms of Minimum inhibitory concentration:-

- ❖ The MIC of the synthesized compounds was determined by applying agar streak dilution method [27].
- ❖ The strains involved Staphylococcus aureus and Bacillus subtilis as Gram (+)ve bacteria; Escherichia coli and Pseudomonas aeruginosa as Gram (-)ve bacteria; Candida albicans and Aspergillus flavus as fungi
- ❖ For anti-bacterial the Ciprofloxacin (100 µg/ml) used as standard, but Fluconazole (100 µg/ml) was used as standard for anti-fungal.
- ❖ A stock solution (100 µg/ml) of the examined compounds in DMSO was prepared and then incorporated in specified quantity of molten sterile.
- ❖ A certain amount of the medium containing tested compound was decanted into a Petri dish to reach a depth of 3-4 mm at 40-50 °C and then, permitted to solidify.
- ❖ The micro-organism suspension was set to take about 10⁵ cfu/ml and smeared to plates with diluted compounds in DMSO to be tested and then, incubated for 24-48 h at 37°C.
- ❖ The MIC was measured until the lowest concentration of the test substance showing no visible growth of bacteria or fungi on the plate.

Anti-oxidant activity screening assay - ABTS method:-

- ❖ In ABTS method; (2 ml, 60 mM) of ABTS + (3 ml, 25 mg/ml) MnO₂ + (5 ml, pH 7, 0.1 M) phosphate buffer was added to investigated compounds.
- ❖ The absorbance was measured at λ₇₃₄ nm for the resultant green-blue solution after the mix was shaken, centrifuged and filtered.
- ❖ After that, (50 ml, 2 mM) the investigated compounds was added to (1:1) methanol/phosphate buffer in spectroscopic grade.
- ❖ The absorbance was detected, and the intensity of color reduction was supposed as inhibition %. The L-ascorbic acid (standard antioxidant) used as a (+) control.
- ❖ Blank sample was run without ABTS and using methanol/phosphate buffer (1:1) in place of tested compounds. However, the ABTS and methanol/phosphate buffer (1:1) used as a negative control [28, 29].

$$I\% = (A_{\text{blank}} - A_{\text{sample}}) / (A_{\text{blank}}) \times 100$$

Where A_{blank} is the absorbance of the control reaction,

A_{sample} is the absorbance in the existence of the testers or standards.

Anti-oxidant screening assay for erythrocyte hemolysis:-

Erythrocytes were gotten from the buffy coat and plasma then, the blood was acquired by cardiac puncture from rats and then collected in heparinized tubes. After that, the mix was washed three times with 10 volumes of 0.15 M NaCl, then, it centrifuged for 10 min at 2500 rpm to attain a regularly packed cell preparation. In this examine system erythrocyte hemolysis was intervened by peroxy radicals [30]. To the same volume of 200 mM of AAPH solution in PBS, a 10% of erythrocytes suspension in pH 7.4 phosphate-buffered saline (PBS) was added to the investigated samples at different concentrations. Then the mix was shaken and incubated at 37 °C for 1 hour. Next, mixture was detached, diluted with 8 volumes of PBS and centrifuged at 2500 rpm for 10 min. The absorbance (A) of the supernatant was detected at 540 nm. Likewise, the mixture was conserved with 8 volumes of distilled water to attain complete hemolysis then, at 540 nm the absorbance (B) of the supernatant attained after centrifugation was determined. The % hemolysis was measured by the following equation:

$$\% \text{ hemolysis} = (1 - A/B) \times 100\%$$

Cell proliferation assay:-

- ❖ By MTT colorimetric assay the compounds inhibitory effects on cell growth was determine [31, 32].
- ❖ The 100 units/ml penicillin and 100µg/ml streptomycin are the antibiotics used under 5% CO₂ at 37 °C for 48 h incubator and seeds in a 96-well plate with density 1.0x10⁴ cells/well [33, 34].
- ❖ Then the incubated cells were conserved with dissimilar concentration of compounds for 24 h. next, 24 h of medicine action, 20 µl of MTT solution at 5 mg/ml was added and incubated for 4 h.
- ❖ After that 100 µl of DMSO was added to each well to dissolve the purple formazan. The colorimetric test was determined by using a plate reader (EXL 800, USA) at absorbance of 570 nm.
- ❖ By using the following equation the % of relative cell viability was measured:

$$A_{570} \text{ of treated samples} / A_{570} \text{ of untreated sample} \times 100.$$

Flotation-separation procedure:-

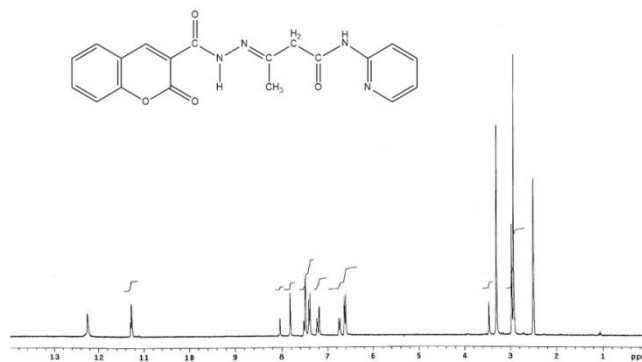
A definite amount of Cd²⁺ and Pb²⁺ solutions was added to the dissolved ligand. The pH of earlier mixture was adjusted with sodium hydroxide and/or nitric acid to reach the preferred concentration. Then, the distilled water was added to 10 mL with in the flotation cell. To confirm complete complexation, the cell was shaken well for 2 min and then 2 mL of oleic acid were added. After that, the cell was inverted upside down 20 times by hand and left 5 min standing for comprehensive flotation. Lastly, the concentration of Cd²⁺ or Pb²⁺ ions remained in the mother liquor was investigated via AAS. The floatability % of Cd²⁺ or Pb²⁺ ions was determined by using the following equation:

$$F \% = (C_i - C_f) / C_i \times 100$$

Where: C_i is initial concentrations; C_f is the final concentrations, of Cd²⁺ or Pb²⁺ ions in the mother liquor, respectively.

Results and Discussion:-**IR and ¹H NMR spectra:-**

In the IR spectrum of H₂L (Table 2), the bands observed at 1603, 689, 1750, 1655, 1675, 3285, 3180 and 3051 cm⁻¹ are attributed to ν(C=N), ν(C=N)_{py}, ν(C=O)₁, ν(C=O)₂, ν(C=O)₃, ν(NH)₁, ν(NH)₂, ν(CH₂) [35-37]. Also, in ¹H NMR spectrum of H₂L there are two signals observed at 11.27 and 12.23 ppm ascribed to the (NH)₁ and (NH)₂ protons, respectively (Scheme 2). There are multiplet signals were showed in 6.60–8.04 ppm region related to the –N=CH– and aromatic protons. There is a sharp signal correlated to protons of (–CH₂) at 3.46 ppm.



Scheme 2. ¹H NMR spectrum of H₂L in DMSO

In $[\text{Hg}(\text{H}_2\text{L})(\text{H}_2\text{O})_2\text{Cl}_2]$ complex the ligand behaved in a neutral bidentate manner coordinating via carbonyl oxygen ($\text{C}=\text{O}$)₃ and azomethine nitrogen ($\text{C}=\text{N}$). This mode of coordination is suggested by the negative shift of both $\nu(\text{C}=\text{O})_3$ and $\nu(\text{C}=\text{N})$ the existence of new bands at 565 and 476 cm^{-1} which ascribed to ($\text{Hg}-\text{O}$) and ($\text{Hg}-\text{N}$) [38], respectively.

Also, in the IR spectrum of $[\text{Mn}(\text{H}_2\text{L})(\text{H}_2\text{O})\text{Cl}_2]$ complex, H_2L behaved as a neutral tridentate ligand chelating via ($\text{C}=\text{N}$), ($\text{C}=\text{O}$)₂ and ($\text{C}=\text{O}$)₃. This mode of complexation was supported by the negative shift of $\nu(\text{C}=\text{N})$, $\nu(\text{C}=\text{O})_2$ and $\nu(\text{C}=\text{O})_3$. The appearance of new bands at the 563 and 467 cm^{-1} that ascribed to $\nu(\text{Mn}-\text{O})$ and $\nu(\text{Mn}-\text{N})$ [38], respectively.

Lastly, in $[\text{Co}(\text{HL})(\text{OAc})(\text{H}_2\text{O})].2\text{H}_2\text{O}$ complex, the ligand behaved as a mononegative tridentate ligand coordinating via ($\text{C}=\text{N}$)_{py}, ($\text{C}=\text{N}$) and ($\text{C}=\text{O}$)₃. This manner of complexation is suggested by the absences of ($\text{C}=\text{O}$)₃ and (NH_2), with immediate appearance of new bands at 1609 and 1275 attributable to ($\text{C}=\text{N}^*$) and ($\text{C}-\text{O}$)_{enolic}, respectively [39]. The appearance of new bands at 554 and 470 cm^{-1} which may be attributed to ($\text{Co}-\text{O}$) and ($\text{Co}-\text{N}$) [38], respectively.

Table 2. Most important IR spectral bands of H_2L and its metal complexes

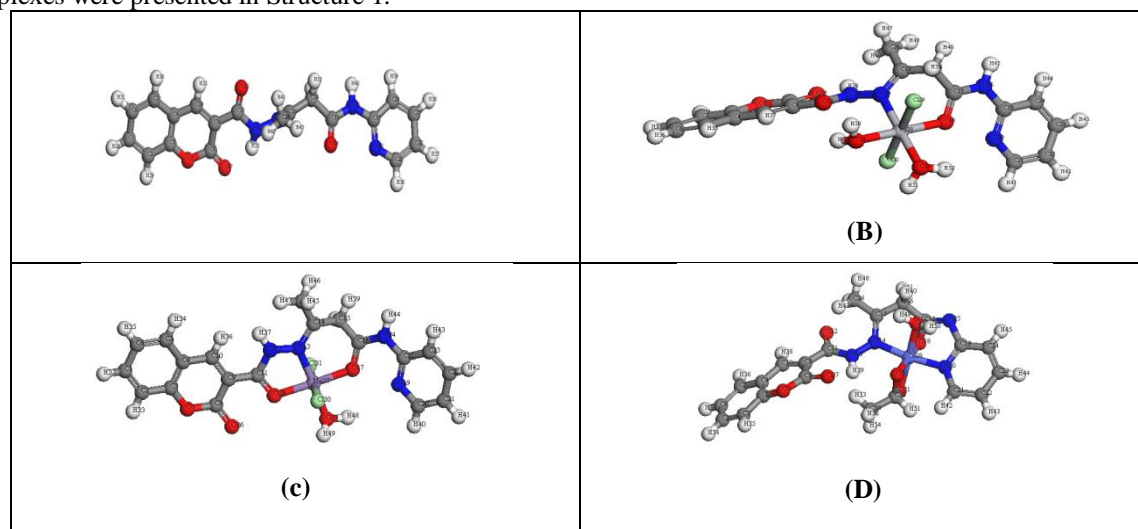
Compound	$\nu(\text{NH})_1$	$\nu(\text{NH})_2$	$\nu(\text{CH}_2)$	$\nu(\text{C}=\text{O})_1$	$\nu(\text{C}=\text{O})_2$	$\nu(\text{C}=\text{O})_3$	$\nu(\text{C}=\text{N})$	$\nu(\text{C}=\text{N})_{\text{py}}$	$\nu(\text{C}=\text{N}^*)$	$\nu(\text{C}-\text{O})_{\text{enolic}}$	$\nu(\text{M}-\text{O})$	$\nu(\text{M}-\text{N})$
1	3285	3180	3051	1750	1655	1675	1603	689	-	-	-	-
2	3314	3189	3051	1752	1660	1649	1597	662	-	-	565	476
3	3285	3184	3047	1750	1643	1638	1592	681	-	-	563	467
4	3263	-	3067	1752	1652	-	1575	754	1609	1275	554	470

Magnetic moments and electronic spectra:-

In $[\text{Co}(\text{HL})(\text{OAc})(\text{H}_2\text{O})].2\text{H}_2\text{O}$ electronic spectrum there are two bands at 17857 and 14084 cm^{-1} attributed to ${}^4\text{T}_{1g} \rightarrow {}^4\text{A}_{2g}(\text{F})$ and ${}^4\text{T}_{1g} \rightarrow {}^4\text{T}_{1g}(\text{P})$ transitions, respectively, in an octahedral configuration [40]. The calculated values of $Dq = 743$, $B = 825$, $\beta = 0.85$ and $\nu_2/\nu_1 = 2.15$ are in good agreement with those stated for octahedral Cobalt (II) complexes. The position of $\nu_1 = 6547 \text{ cm}^{-1}$ is calculated theoretically [40]. Moreover, the value of magnetic moment that equal to 5.1 BM is consistent with octahedral geometry around the Cobalt (II) ion.

Geometry optimization with DFT method:-

The geometry of new molecular compounds resulting from the interaction between the H_2L and several metal cations can be predicted by using DFT method. The molecular structure beside with atom numbering of H_2L and its metal complexes were presented in Structure 1.



Structure 1. Molecular modeling of (A) H_2L , (B) $[\text{Hg}(\text{H}_2\text{L})(\text{H}_2\text{O})_2\text{Cl}_2]$, (c) $[\text{Mn}(\text{H}_2\text{L})(\text{H}_2\text{O})\text{Cl}_2]$, (D) $[\text{Co}(\text{HL})(\text{OAc})(\text{H}_2\text{O})].2\text{H}_2\text{O}$

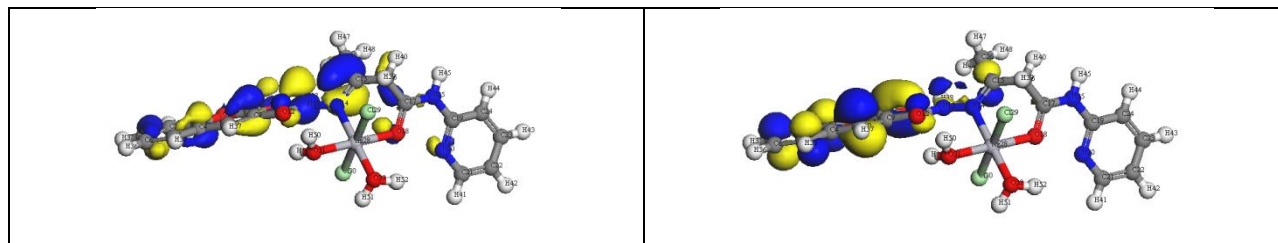
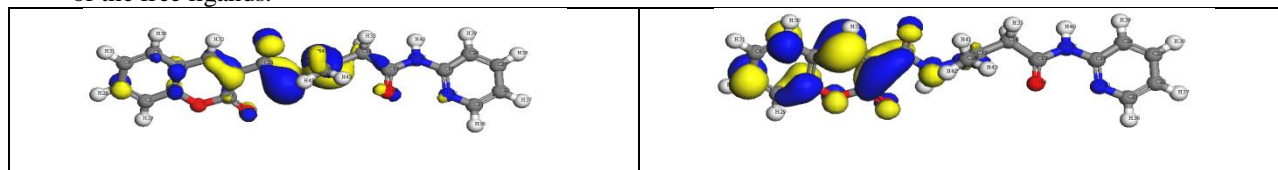
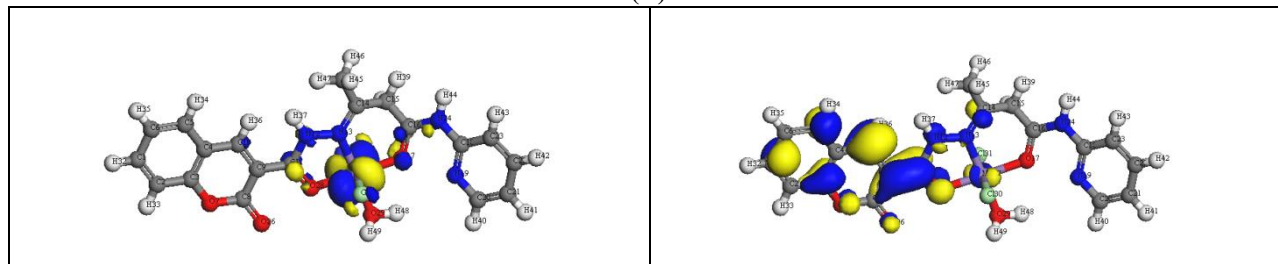
Molecular parameters:-

The Quantum chemical parameters such as E_{HOMO} and E_{LUMO} of prepared compounds were estimated. Moreover, dipole moment, total energy and binding energy were calculated as shown in Table 3. From the outcome data we can assumed that:

Table 3:- The molecular parameters of the ligand and its complexes.

Compound	Total Energy (Ha)	Binding Energy (Ha)	Dipole moment (debye)	HOMO (eV)	LUMO (eV)
1	-1254.429809	-8.3941386	3.8916	-5.523	-3.075
2	-2556.664661	-9.4867640	4.2017	-6.265	-3.661
3	-2373.548254	-9.3038517	7.0691	-4.463	-3.518
4	-1726.739102	-10.3842915	1.1535	-4.169	-3.421

1. The negative values of E_{HOMO} and E_{LUMO} indicated the stability of prepared complexes (Figure 1).
2. The lower values of E_{HOMO} indicated the molecule donating electron ability is small. On opposing, the larger E_{HOMO} suggested that the molecule is a good electron donor.
3. The binding energy of complexes was greater than free ligand that showed a great stability of the complexes.
4. The ligand exhibited higher value of dipole moment than prepared complexes that enhanced the potent activities of the free ligands.

**(B)****(C)**

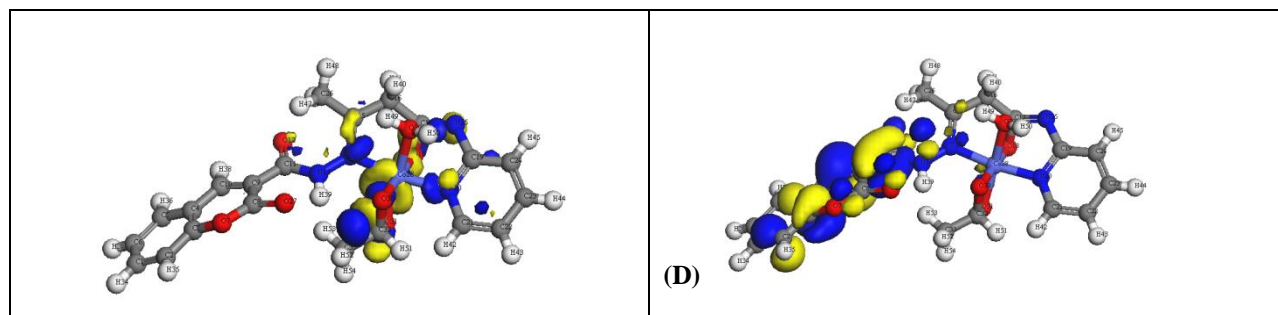


Fig. 1:- The HOMO and LUMO of (A) H_2L , (B) $[Hg(H_2L)(H_2O)_2Cl_2]$, (C) $[Mn(H_2L)(H_2O)Cl_2]$, (D) $[Co(HL)(OAc)(H_2O)].2H_2O$

Molecular electrostatic potential (MEP) of H_2L :-

The MEP was reflected a good descriptor sites for nucleophilic and electrophilic attack [41]. In the current study, 3D plots of MEP were drawn for the ligand and their metal complexes (Figure 2). From the MEP, the electron-rich area has red colour (favour site for electrophilic attack). However, the electron-poor area has blue colour (favour site for nucleophilic attack) [42]. But, the green area indicated to the neutral electrostatic potential region.

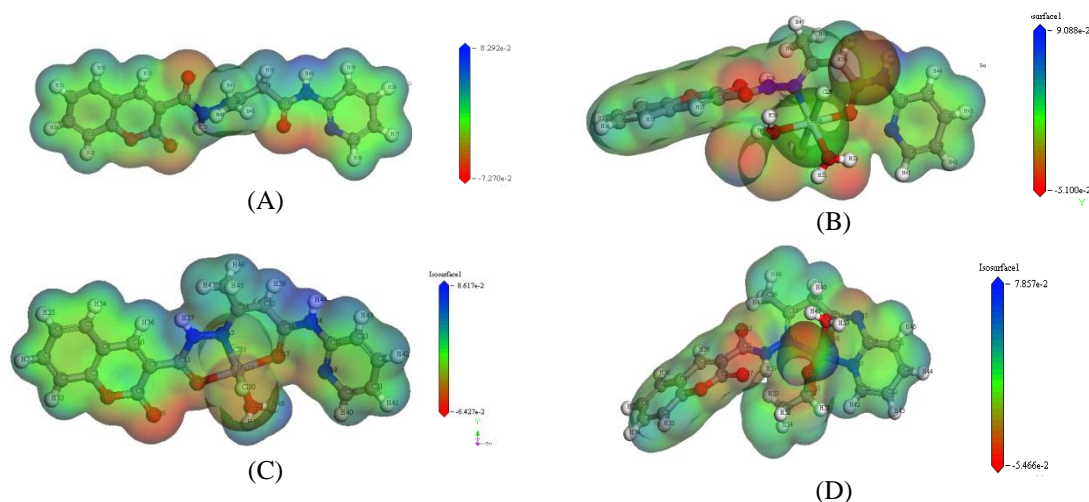


Fig. 2:p Molecular electrostatic potential map for (A) H_2L , (B) $[Hg(H_2L)(H_2O)_2Cl_2]$, (C) $[Mn(H_2L)(H_2O)Cl_2]$, (D) $[Co(HL)(OAc)(H_2O)].2H_2O$.

Biological activity:-

The biological activity of Coumarin derivatives was encouraged us to assume systematic studies on their complexation affinity and test their abilities beside economically vital fungal and bacteria [43, 44].

Antifungal activity:-

The results revealed that the ligand and its metal complexes have an important activity against *Aspergillus flavus* and *Candida albicans* (Table 4). The H_2L and Mn(II) complex are more potent against *Aspergillus flavus* than *Candida albicans* in comparison with the standard drug Fluconazole [45].

Antibacterial activity:-

The investigated compounds along with Ciprofloxacin (standard drug) and DMSO (solvent control) were screened individually for their antibacterial activity [46-48]. The activity of the tested compounds was matched to the activity of Ciprofloxacin as a standard antibiotic. The MIC values showed that H_2L and Mn(II) complex have the highest antibacterial activity (Table 4).

Table 4. Antibacterial and antifungal activities in terms of MIC ($\mu\text{g/mL}$)

Compound	E. coli	P. aeruginosa	S. aureus	B. subtilis	C. Albicans	A. flavus
Ciprofloxacin	1.56	0.78	1.56	0.39	-	-
Fluconazole	-	-	-	-	1.56	0.78
1	1.17	0.58	1.17	0.78	1.56	1.17
2	37.5	25	9.37	4.68	12.5	6.25
3	1.56	0.78	1.17	0.58	2.34	1.56
4	>100	50	25	18.75	37.5	25

The antioxidant activity of ligands and their metal complexes:-

The antioxidant activity of the tested compounds was estimated using ABTS assay [49]. All tested compounds have low antioxidant activity except H_2L and Mn(II) complex demonstrated the maximum antioxidant activity in comparison with standard ascorbic-acid. Additionally, the anti-oxidant activity of tested compounds was established for erythrocyte hemolysis. All the tested compounds demonstrated weak anti-oxidative activity in the hemolysis assay, but Mn(II) complex has well effects (Table 5, 6).

Table 5:- Anti-oxidant assays by ABTS method

Method	ABTS	
	Abs(control)-Abs(test)/Abs(control)x100	
Compounds	Absorbance of samples	% inhibition
Control of ABTS	0.510	0%
Ascorbic-acid	0.055	89.2%
1	0.077	84.9%
2	0.223	56.3%
3	0.078	84.7%
4	0.245	52.0%

Table 6:- Anti-oxidant assays by erythrocyte hemolysis

Compounds	Erythrocyte hemolysis	
	A/B x 100	
	Absorbance of samples (A)	% hemolysis
Absorbance of H_2O (B)	0.896	---
Ascorbic-acid	0.042	4.7%
1	0.116	12.9%
2	0.395	44.1%
3	0.089	9.9%
4	0.389	43.4%

The cytotoxicity of H_2L and its metal complexes on HCT-116 cell line:-

The cytotoxicity examine of the investigated compounds against human colorectal carcinoma cells lines (HCT) were demonstrated in Table 7. The data detected that the ligand ($\text{IC}_{50} = 4.8 \mu\text{g/ml}$) and Mn(II) complex ($\text{IC}_{50} = 5.5 \mu\text{g/ml}$) were established a greatly inhibitory effect than the other tested compounds. Conversely, Co(II) complex has greater IC_{50} value (47.8 $\mu\text{g/ml}$) revealed almost no activity [50].

Table 7:- Cytotoxicity (IC_{50}) of tested compounds on HCT-116 cell line.

Compounds	In vitro Cytotoxicity IC_{50} ($\mu\text{g/ml}$)
5FU	5.2
1	4.8
2	25.7
3	5.5
4	47.8

Ion-flotation separation:-

Influence of initial pH:-

The effect of initial pH were performed on the floatability of metal ions (2×10^{-4} mol.L⁻¹) using 1×10^{-3} mol.L⁻¹ of HOL and 2×10^{-4} mol.L⁻¹ of H₂L. The results showed that, the maximum floatability were reached in the pH range (6-10) for Pb²⁺ and (5-10) for Cd²⁺ ions (Figure 3). This enables the use of the H₂L for the separation of metal ions from different media.

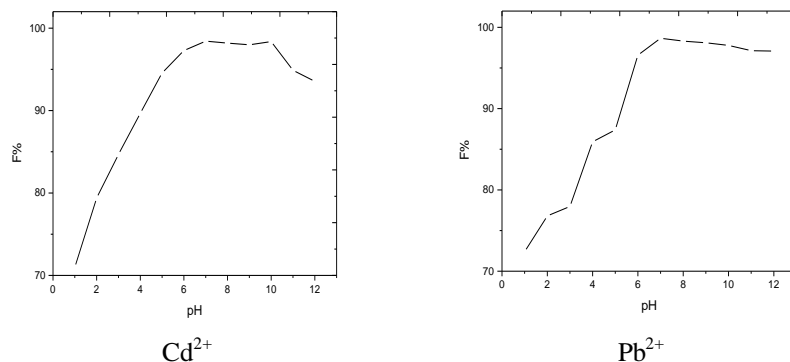


Fig. 3:- Influence of pH on the floatability of 2×10^{-4} mol.L⁻¹ Cd²⁺ and Pb²⁺ ions using 2×10^{-4} mol.L⁻¹ of ligand and 1×10^{-3} mol.L⁻¹ HOL.

Influence of initial metal concentration:-

Attempts to float various concentrations of Cd²⁺ and Pb²⁺ ions using 2×10^{-4} mol.L⁻¹ of H₂L and 1×10^{-3} mol.L⁻¹ HOL at pH~7 were carried out. The results displayed that the maximum flotation efficiency (~100%) of Cd²⁺ and Pb²⁺ ions was achieved and rested constant for the H₂L whenever the ratio of M:L is (1:1) (Figure 4). The chelating agent presented quantitative separation of Cd²⁺ and Pb²⁺ ions (~100%) which attributed to the presence of sufficient quantities of H₂L to bind all Cd²⁺ and Pb²⁺ ions.

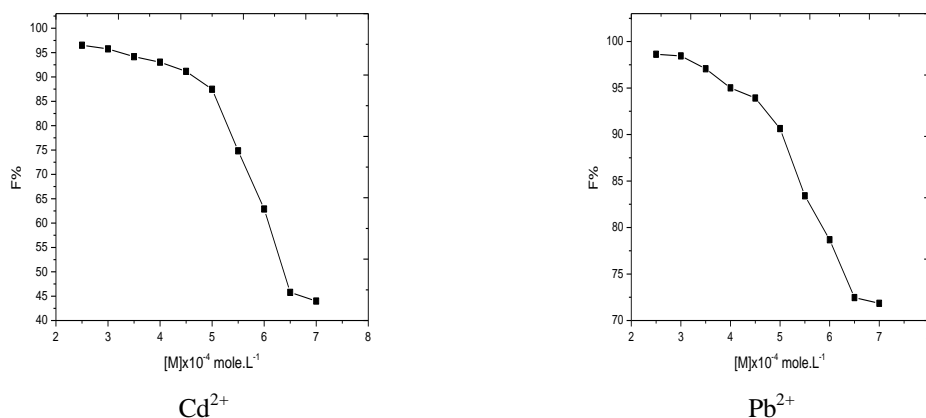


Fig. 4:- Floatability of different concentrations of Cd²⁺ and Pb²⁺ ions using 2×10^{-4} mol.L⁻¹ of prepared ligand and 1×10^{-3} mol.L⁻¹ HOL at pH ~7

Influence of ligand concentration:-

The collecting ability of H₂L to Cd²⁺ and Pb²⁺ ions was experienced using 1×10^{-3} mol.L⁻¹ HOL at pH~7. The outcomes data showed that, the floatability of Cd²⁺ and Pb²⁺ ions increases sharply reaching its maximum value (~100%) at M:L ratio of (1:1) (Figure 5). Additional H₂L has no opposing effect on the flotation method, therefore 2×10^{-4} mol.L⁻¹ of H₂L was used throughout.

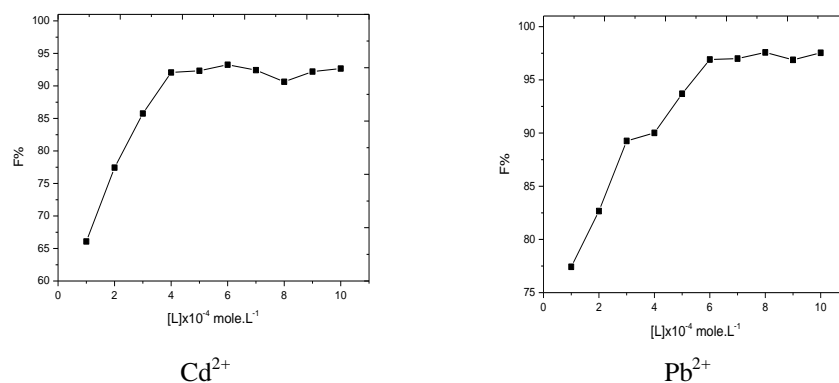


Fig. 5:- Floatability of 2×10^{-4} mol.L⁻¹ Cd²⁺ and Pb²⁺ ions using different concentrations of prepared ligand and 1×10^{-3} mol.L⁻¹ HOL at pH ~7

1.1.1. Influence of surfactant concentration

Trials were accepted to float Cd²⁺ and Pb²⁺ ions with HOL alone, however the recovery did not exceed 27.5 %. Hence, further experiments were done to float 2×10^{-4} mol.L⁻¹ Cd²⁺ and Pb²⁺ ions in the existence of 2×10^{-4} mol.L⁻¹ of H₂L and various concentrations of HOL (1×10^{-3} - 5×10^{-2} mol.L⁻¹) at pH~7. The outcomes data showed that the HOL concentration in 1×10^{-3} - 9×10^{-3} mol.L⁻¹ range, high floatation % of Cd²⁺ and Pb²⁺ was reached (Figure 6). The partial separation of Cd²⁺ or Pb²⁺ ions at larger surfactant concentration assignable to the fact that the surfactant improved the particles state, Cd²⁺ and Pb²⁺ ligand precipitates, from coagulation precipitation via coagulation flotation to re-dispersion with an increase in the added amount of HOL [51]. Moreover, at great surfactant concentration, poor flotation was observed because of the formation a stable hydrate micelle coating on the solid surface or, by forming hydrated envelope of surfactant on the air bubble surface [52, 53].

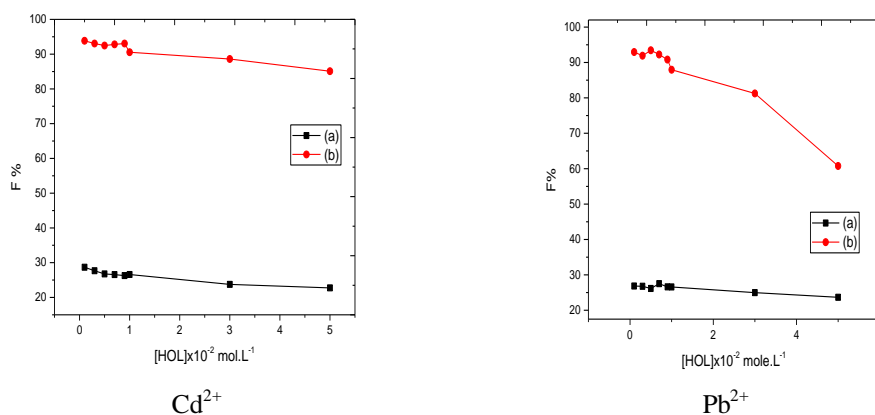


Fig. 6. Floatability of 2×10^{-4} mol.L⁻¹ Cd²⁺ and Pb²⁺ ions using different concentrations of HOL in the absence (a) and presence (b) of 2×10^{-4} mol.L⁻¹ of prepared ligand at pH ~7

Influence of temperature:-

The Mixture containing Cd²⁺ or Pb²⁺ ions, H₂L and other solution involving HOL were either heated in a water bath or cooled in an ice bath at the identical temperature. The HOL solution was rapidly poured into Cd²⁺ or Pb²⁺ ions solution. The mixture was bring together to the flotation cell. The outcome data shown the maximum flotation (~100%) of Cd²⁺ and Pb²⁺ ions lie in 15-80°C range (Figure 7). The decrease in separation by increasing temperature more than 80°C due to the solubility of the precipitate increase and the instability of the foam giving rise to partial dissolution of the precipitate and insufficient foam constancy to delay the precipitate [54].

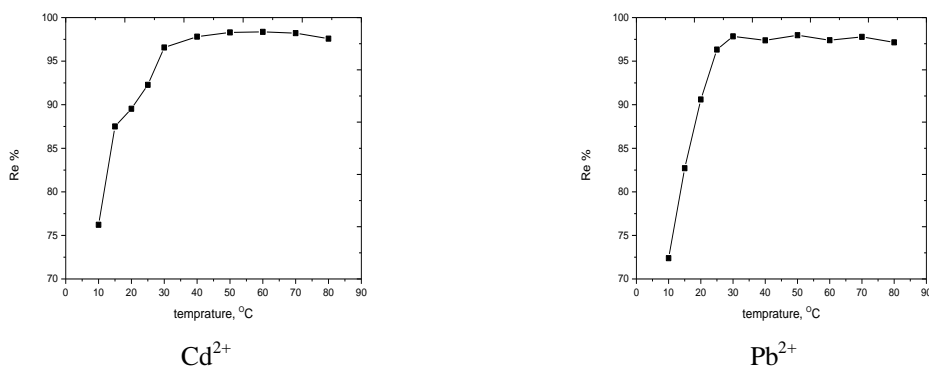


Fig. 7:- Floatability of 2×10^{-4} mol.L⁻¹ Cd²⁺ and Pb²⁺ ions at different temperatures using 2×10^{-4} mol.L⁻¹ of prepared ligand and 1×10^{-3} mol.L⁻¹ HOL at pH ~7

Effect of presence of foreign ions

The percentage of removal of Cd²⁺ and Pb²⁺ ions from a solution of pH 7 containing 30 mg.L⁻¹ of H₂L was performed in the existence of high concentrations of different cations and anions. The anions used as chlorides while, the cations used as Na⁺ or K⁺ salts. The suitable quantities for each ion, giving an error ($\pm 4\%$) in the removal efficiency of Cd²⁺ and Pb²⁺ ions (Table 8). The data indicated that all the foreign ions with comparatively high concentrations have no opposite effect on the flotation of Cd²⁺ and Pb²⁺.

Table 8:- Effects of the foreign ions on the removal percentage of the examined metal ions

Ion	Interference/analyte ratio (mg L ⁻¹)	Re % Cd(II)	Re % Pb(II)
Na ⁺	35	97.2	97.8
K ⁺	35	98.8	99.8
Mg ²⁺	25	96.6	98.3
Ca ²⁺	20	94.3	95.7
Cl ⁻	35	95.7	96.9
SO ₄ ²⁻	35	97.9	97.1
HCO ₃ ⁻	15	99.5	96.4
CH ₃ COO ⁻	30	95.4	98.1

[M = 2×10^{-4} mol.L⁻¹; Ligand = 2×10^{-4} mol.L⁻¹; HOL = 1×10^{-3} mol.L⁻¹; pH = 7]

Application:-

Numerous experiments were done to study the applicability of the proposed method of recover Cd²⁺ and Pb²⁺ ions spiked to 1L of aqueous samples. The flotation experiments were done at pH 7 using 50 mL filtered sample solutions. The outcomes data shown that the recovery was acceptable and measureable under the suggested conditions of the applied flotation method (Table 9).

Table 9:- Recovery of studied metal ions from some water samples

Water samples (location)	Cd ²⁺		Pb ²⁺	
	Added metal (mg.L ⁻¹)	Re %	Added metal (mg.L ⁻¹)	Re %
Mansoura	10.15	87.49	15	92.47
Bilqas	10.15	89.18	15	93.20
Alexandria	10.15	87.54	15	92.92
Sharm El-Shiekh	10.15	84.32	15	95.10

[Ligand = 2×10^{-4} mol.L⁻¹; HOL = 1×10^{-3} mol.L⁻¹; pH = ~7]

Proposed flotation mechanism:-

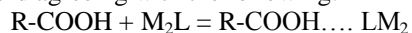
The flotation mechanism of analyte-ligand precipitates was proposed depending on the following facts:

Cd²⁺ and Pb²⁺ ions reacted with H₂L in a M:L ratio of (1:1) to produce the M₂L complex consistent with this equation:



H₂L has several electronegative atoms such as nitrogen and oxygen in the form of C=N, C=O and NH functional groups that can form hydrogen bonds.

The oleic acid began to dissociate at $\text{pH} > 5.2$ [54] and the % of different forms of HOL were detected by IR analysis (Table 10). The IR spectra of oleic acid with changing pH indicated that at $1300\text{-}1800\text{ cm}^{-1}$, there are significant bands of COOH , COO^- and COO^-Na^+ [55]. These results agree with those reported [56] where, the $\text{C}=\text{O}$ stretching band of oleic acid at 1705 cm^{-1} is shifted on ionization to bands in $1520\text{-}1540\text{ cm}^{-1}$ range for sodium oleate. Thus, oleic acid can performance together with other structures, via hydrogen bonding, either in (R-COOH) or (R-COO^-) forms depending on the pH of the medium and agreeing with the following:



The combination of oleic acid surfactant with the cadmium-ligand or lead-ligand chelate providing hydrophobic aggregates that float with the assistance of air bubbles to the solution surface [57].

Table 10:- Different forms of oleic acid determined by spectrophotometric.

pH	(%)			Total
	HOL	Ol ⁻	NaOL	
5.2	100	0.0	0.0	100
8.0	6.5	34.2	0.0	100
8.2	38.5	57.7	3.8	100
9.0	13.6	68.2	18.2	100
11.5	0.0	80.0	20.0	100
12.0	0.0		52.2	47.8

References:-

- Casley-Smith, J. R.; Morgan, R. G.; Piller, N. B. *NEJM* **1993**, 329, 16, 1158–63.
- Schäfer, F. P. *Dye Lasers*, 3rd ed.; Berlin: Springer-Verlag, **1990**.
- Duarte, F. J.; Hillman, L. W. *Dye Laser Principles*; Academic press: New York, **1990**.
- Duarte, F. J. *Tunable Laser Optics*; Elsevier-Academic: New York, **2003**.
- Corey, E. J.; Enders, D. *Chemische. Berichte.* **1978**, 111, 1337–1361. doi:10.1002/cber.19781110413.
- Ritter, J. K.; Chen, F.; Sheen, Y. Y.; Tran, H. M.; Kimura, S.; Yeatman M. T.; Owens I. S. *J Biol Chem.* **1992**, 267, 5, 3257–61.
- Link, K. P. *Circulation* **1959**, 19, 97–107. doi:10.1161/01.CIR.19.1.97.
- Liu, H. Extraction and Isolation of Compounds from Herbal Medicines. In: Willow, J. and Liu, H. *Traditional Herbal Medicine Research Methods*. John Wiley and Sons, Inc. **2011**.
- Farinola, N.; Piller, N. *LYMPHATIC RESEARCH AND BIOLOGY* **2005**, 3, 2, 81-86. doi:10.1089/lrb.2005.3.81.
- International Programme on Chemical Safety. "Brodifacoum (pesticide data sheet)". Retrieved 2006-12-14
- Laposata, M.; Van Cott, E. M.; Lev, M. H. *N Engl J Med.* **2007**, 356, 2, 174-82.
- Bye, A.; King, H. K. *Biochemical Journal* **1970**, 117, 237-45.
- Montagner, C.; De Souza, S. M.; Groposoa, C.; Delle Monache, F.; Smânia, E. F.; Smânia Jr. A. *Zeitschrift für Naturforschung* **2008**, C **63**, (1-2), 21–8.
- Weber, U. S.; Steffen, B; Siegers, C. P. *Europe PMC* **1998**, 99, 2, 193–206.
- Oliveira, P.F.M.; Baron, M.; Chamayou, A.; André-Barrès, C.; Guidetti, B.; Baltas, M. *RSC Adv.* **2014**, 4, 100. doi:10.1039/c4ra10489g.56736–56742.
- Ibrahim, K.; Zaky, R.; Gomaa, E.; El-Hady, M. *Research Journal of Pharmaceutical, Biological and Chemical Sciences* **2011**, 2, 3, 391–404.
- Ibrahim, K.; Zaky, R.; Gomaa, E.; El-Hady, M. *Anaele Universitatii din Bucuresti* **2011**, 20, 149–154.
- El-Hady, M.; Zaky, R.; Ibrahim, K.; Gomaa, E. *Journal of Molecular Structure* **2012**, 1016, 169–180.
- Ibrahim, K.; Gomaa, E.; Zaky, R.; El-Hady, M. *American Journal of Chemistry* **2012**, 2, 2, 23–26.
- Ibrahim, K.; Zaky, R.; Gomaa, E.; El-Hady, M. *Spectrochimica Acta Part A* **2013**, 107, 133–144.
- Delley, B. *Phys Rev.* **2002**, 65, 85403–8509.
- Modeling and Simulation Solutions for Chemicals and Materials Research, Materials Studio (Version 5.0), Accelrys software Inc., San Diego, USA. Available online at: www.accelrys.com **2009**.
- Hehre, W. J.; Radom, L.; Schlyer, P. V. R.; Pople, J. A. *Ab Initio Molecular Orbital Theory*, Wiley, New York **1986**.
- Kessi, A.; Delley, B. *International Journal of Quantum Chemistry* **1998**, 68, 135–144.

25. Hammer, B.; Hansen, L. B.; Nørskov, J. K. *Phys. Rev. B* **1999**, 59, 7413–7421.
26. Matveev, A.; Stauffer, M.; Mayer, M.; Rösch, N. *Int. J. Quantum Chem* **1999**, 75, 863–873.
27. Hawkey, P. M.; Lewis, D. A.; Oxford University Press: United Kingdom, **1994**, 181–194.
28. Mosmann, T. *Journal of Immunological Methods* **1983**, 65, 55–63.
29. Lissi, E.; Modak, B.; Torres, R.; Escobar, J.; Urzua, A. *Free Radical Res* **1999**, 30, 471–477.
30. El-Gazzar, A.; Youssef, M.; Youssef, A.; Abu-Hashem, A.; Badria, F. *Eur J Med Chem* **2009**, 44, 609–624.
31. Aeschlach, R.; Loliger, J.; Scott, C.; Murcia, A.; Butler, J.; Halliwell, B.; Aruoma, I. *Food Chem. Toxicol* **1994**, 32, 31–36.
32. Denizot, F.; Lang, R. J. *Immunol. Methods* **1986**, 89, 271–277.
33. Mauceri, H.; Hanna, N.; Beckett, M.; Gorski, D.; Staba, M.; Stellato, K.; Bigelow, K.; Heimann, R.; Gately, S.; Dhanabal, M.; Soff, G.; Sukhatme, V.; Kufe, D.; Weichselbaum, R. *Nature* **1998**, 394, 287–291. doi: 10.1038/28412.
34. Morimoto, Y.; Tanaka, K.; Iwakiri, Y.; Tokuhira, S.; Fukushima, S.; Takeuchi, Y. *Biol. Pharm Bull* **1995**, 18, 417–422.
35. Ibrahim, K.; Gabr, I.; Abu El-Reash, G.; Zaky, R. *Monatsh Chem* **2009**, 140, 625–632. doi: 10.1007/s00706-009-0106-x.
36. Ibrahim, K.; Zaky, K.; Gomma, E.; El-Hady, M. *Res J Pharm Biol Chem Sci* **2011**, 2, 391–404.
37. Pretsch, E.; Bühlmann, P.; Badertscher, M. 4th; Berlin: Heidelberg, **2009**.
38. Zaky, R.; Yousef, T. *Journal of Molecular Structure* **2011**, 1002, 76–85.
39. Zaky, R. Taylor & Francis Group, LLC **2011**, 186, 365–380. doi:10.1080/10426507.2010.503207
40. Cotton, F. A.; Wilkinson, G.; Murillo, C. A.; Bochmann, M. *Advanced Inorganic Chemistry*, 6th ed., John Wiley & Sons Inc. **2003**.
41. Zalaoglu, Y.; Ulgen, A.; Terzioglu, C.; Yildirim, G. *Fen Bilimleri Dergisi* **2010**, 14, 66–76.
42. Tanak, H.; Köysal, Y.; Işık, Ş.; Yaman, H.; Ahsen, V. *Bull. Korean Chem* **2011**, 32, 673–680.
43. Filipović, N.; Borrmann, H.; Todorović, T.; Borna, M.; Spasojević, V.; Sladić, D.; Novaković, I.; Andjelković, A. *Inorganica Chimica Acta* **2009**, 362, 1996–2000.
44. Thimmaiah, N.; Chandrappa, T.; Jayarama, R. *Polyhedron* **1984**, 3, 1237–1239. doi:10.1016/S0277-5387(00)84669-0.
45. Nagar, R. *Journal of Inorganic Biochemistry* **1990**, 40, 349–356.
46. Johari, R. B.; Sharma, R. C. *J Indian Chem Soc.* **1988**, 65, 793–794.
47. Abd El-Wahab, Z.; El-Sarrag, M. *Spectrochimica Acta A* **2004**, 60, 271–277.
48. Panchal, P.; Parekh, H.; Patel, M.; *Toxicol. Environ. Chem* **2005**, 87, 313–320.
49. Kostova, I.; Saso, C. *Curr. Med. Chem* **2013**, 20, 4609–4632.
50. Yousef, A.; Badria, F.; Ghazy, S.; El-Gammal, O.; Abu El-Reash, G. *Medicine and Medical Sci* **2011**, 3, 37–46.
51. Ghazy, S. E.; Samra, S. E.; Mahdy, A. M.; El-Morsy, S. M. *Anal. Sci.* **2006**, 22, 377–382.
52. Klassen, V. I.; Mokrousov, V. A.; Butterworths: London **1963**.
53. Ghazy, S. E.; Mostafa, G. A. *Bull. Chem. Soc. Jpn.* **2001**, 74, 1273–1278.
54. Ghazy, S. E.; Kabil, M. A. *Bull. Chem. Soc. Jpn.* **1994**, 67, 474–478.
55. Ghazy, S. E.; Rakha T. H.; El-Kady, E. M.; El-Asmy A. A. *Indian J. Chem. Technol* **2000**, 7, 178–182.
56. Pol'kin, S. I.; Berger, G. S.; Revazashavili, I. B.; Shchepkina, M. M. *Izv. Vyssh. Ucheb. Zaved. Tsvet. Met* **1968**, 11, 6–11.
57. Ramachandra, R. S. *Surface Chemistry of Froth Flotation, Vol. 2 Reagents and Mechanisms*, 2nd ed.; Kluwer Academic / Plenum Publishers: